Polyhedron 102 (2015) 773–781

Contents lists available at ScienceDirect

Polyhedron

journal homepage: www.elsevier.com/locate/poly

Synthesis, characterization and anticancer activity of gold(III) complexes with (1*R*,2*R*)-(−)-1,2-diaminocyclohexane

Khalid H. Omer [a], Adam A. Seliman [a], Muhammad Altaf [b], Naike Casagrande [c], Donatella Aldinucci [c], Saleh Altuwaijri [d], Anvarhusein A. Isab [a,*]

[a] Department of Chemistry, King Fahd University of Petroleum and Minerals, Dhahran 31261, Saudi Arabia
[b] Center of Research Excellence in Nanotechnology (CENT), King Fahd University of Petroleum and Minerals, Dhahran 31261, Saudi Arabia
[c] Department of Experimental Oncology 2, CRO Aviano National Cancer Institute, Aviano, PN, Italy
[d] Clinical Research Laboratory, SAAD Research Development Center, SAAD Specialist Hospital, Al-Khobar 31952, Saudi Arabia

ARTICLE INFO

Article history:
Received 12 August 2015
Accepted 8 October 2015
Available online 30 October 2015

Keywords:
(1*R*,2*R*)-(−)-1,2-diaminocyclohexane
Gold(III) complexes
X-ray crystallography
L-540
Cancer cell line

ABSTRACT

Two gold(III) complexes, [(DACH)$AuCl_2$]Cl (**1**) and [$(DACH)_2Au$]Cl_3 (**2**), derived from (1*R*,2*R*)-(−)-1,2-diaminocyclohexane and sodium tetrachloroaurate dihydrate, $NaAuCl_4{\cdot}2H_2O$, were synthesized and fully characterized using elemental analysis and different physical methods, such as FTIR, ^1H NMR, ^{13}C NMR, solid-state NMR and X-ray crystallography. The data confirm the coordination of the DACH ligand to the gold(III) metal centre through its nitrogen atoms. According to *in vitro* cytotoxic studies, complex **2** was more effective against the three human tumor cell lines evaluated (the ovarian cancer cell line A2780, its cisplatin-resistant clone A2780cis and the classical Hodgkin lymphoma cell line L-540). The fold-resistance of the A2780 and A2780cis cells to cisplatin was about twofold lower for both gold(III) complexes.

1. Introduction

One of the most important areas of study in contemporary bioinorganic chemistry is the development of new metal-based drugs [1–11]. Despite the successful use of cisplatin as a chemotherapy agent [12], side effects and resistance have been observed [13]. The use of gold in anti-rheumatic treatment supports its pharmaceutical importance [14–17]. Recent studies have shown that several gold(III) complexes are highly cytotoxic against different tumor cells [18–21]. Oxaliplatin is considered one of the most promising platinum-based drugs, prepared from (1*R*,2*R*)-(−)-1,2-diaminocyclohexane and a labile oxalate ligand [22,23]. Interactions of gold(III) complexes with biomolecules, such as sulfur-containing amino acids, thiols or thioethers, are thought to be the cause of the cytotoxic effect of the gold(III) complexes [24]. The toxic effects arise due to the coordination of the thiol and thioether groups of the side chains in proteins, peptides and amino acids, followed by the reduction of gold(III) to gold(I), then subsequently to toxic gold(0) [25–28]. The electrochemistry of the interaction of guanosine-5-phosphate with gold(III) ethylenediamine complexes was studied by Zhu et al. [29]. The interaction of the dipeptide Gly-Met with gold(III) ethylenediamine showed the formation of Gly-Met sulfoxide along with a free ethylenediamine ligand through a two-step decomposition reaction [30]. The substitution and reduction steps for the reaction of some gold(III) complexes with the sulfur containing biomolecules L-cysteine, L-methionine and glutathione were studied in detail by Durović et al. [31].

In this work, two potential anticancer gold(III) complexes of (1*R*,2*R*)-(−)-1,2-diaminocyclohexane were synthesized and characterized, and their anticancer activities *in vitro* were evaluated.

2. Experimental work

2.1. Chemicals

Sodium tetrachloroaurate(III) dihydrate, and (1*R*,2*R*)-(−)-1,2-diaminocyclohexane (DACH) were obtained from Sigma–Aldrich, USA. Absolute ethanol was obtained from Merck, D_2O was purchased from Alfa Aesar (see Scheme 1).

2.2. Synthesis of complexes

2.2.1. Synthesis of [(1*R*,2*R*)-(−)-1,2-(DACH)$AuCl_2$]Cl

[(1*R*,2*R*)-(−)-1,2-(DACH)$AuCl_2$]Cl (**1**) was synthesized by the direct mixing of $NaAuCl_4{\cdot}2H_2O$ with (1*R*,2*R*)-(−)-1,2-diaminocyclohexane (DACH) in alcoholic media, as previously described [32].

* Corresponding author.
E-mail address: aisab@kfupm.edu.sa (A.A. Isab).

http://dx.doi.org/10.1016/j.poly.2015.10.029
0277-5387/

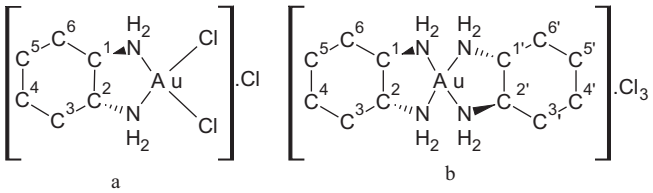

Scheme 1. Chemical structures of (a) $[(DACH)AuCl_2]Cl$ and (b) $[(DACH)_2Au]Cl_3$.

Table 1
Elemental data and melting points for the synthesized complexes.

Complex	Melting point (°C)	Found (calc.) %		
		H	C	N
1	172 decomp.	4.02(3.97)	16.4(15.88)	6.47(6.17)
2	176 decomp.	5.24(5.96)	24.75(23.85)	9.57(9.27)

First, 200 mg (0.5 mmol) $NaAuCl_4{\cdot}2H_2O$ were dissolved using absolute ethanol, 57 mg (0.5 mmol) of (1*R*,2*R*)-(−)-1,2-diaminocyclohexane (DACH) were dissolved in absolute ethanol in a separate beaker, and the second solution was then added dropwise with gentle stirring to the first solution. After a clear solution was obtained, the solution was maintained under refrigeration and after a few days yellow crystals were collected and used for single crystal X-ray diffraction and elemental analysis (Table 1).

2.2.2. Synthesis of [(1R,2R)-(−)-1,2-(DACH)$_2$Au]Cl$_3$

$[(1R,2R)\text{-}(-)\text{-}1,2\text{-}(DACH)_2Au]Cl_3$ (**2**) was synthesized by directly mixing one equivalent of $Na[AuCl_4]{\cdot}2H_2O$ with two equivalents of the diamine ligand in alcoholic media using a previously described method [33]. First, 200 mg (0.5 mmol) of $NaAuCl_4{\cdot}2H_2O$ were dissolved in absolute ethanol, 114 mg (1.0 mmol) of (1*R*,2*R*)-(−)-1,2-diaminocyclohexane (DACH) were dissolved in absolute ethanol in a separate beaker, and the second solution was then added dropwise with gentle stirring to the first solution. The white crystals that formed were collected, washed and used for single crystal X-ray diffraction and elemental analysis (Table 1).

2.3. Solution NMR measurements

All NMR measurements were performed using a JEOL JNM-LA 500 NMR spectrometer. The ^{13}C NMR resonance spectra were obtained with ^{1}H broadband decoupling at a frequency of 125.65 MHz, and they were referenced relative to TMS; the spectral conditions were 32 k data points, 0.963 s acquisition time, 1.00 s pulse delay and a 45° pulse angle. The proton NMR spectra were obtained at a frequency of 500.00 MHz. The ^{1}H and ^{13}C NMR chemical shifts of the free ligand and both complexes are given in Tables 2 and 3.

Table 2
^{1}H NMR for the synthesized gold(III) complexes and free (1*R*,2*R*)-(−)-1,2-diaminocyclohexane in D_2O solvent.

Compound	^{1}H (δ in ppm)				
	H1,H2	H3,H6 (eq)	H3,H6 (ax)	H4,H5 (eq)	H4,H5 (ax)
1(*R*),2(*R*)-DACH	2.19*m*	1.69*m*	1.54*m*	1.13*m*	0.99*m*
1	2.97*m*	2.07*m*	1.54*m*	1.36*m*	1.04*m*
2	3.02*m*	2.12*m*	1.55*m*	1.47*m*	1.09*m*

m: multiplet.

Table 3
^{13}C NMR for the synthesized gold(III) complexes and free (1*R*,2*R*)-(−)-1,2-diaminocyclohexane in D_2O solvent.

Compound	^{13}C (δ in ppm)		
	C1,C2	C3,C6	C4,C5
1(*R*),2(*R*)-DACH	56.8	34.1	25.4
1	65.6	33.0	23.9
2	64.3	32.8	23.9

Table 4
Solid-state NMR for the synthesized gold(III) complexes.

Compound	C1,C2	C3,C6	C4,C5
1	68.5	36.9	26.5
2	66.9	36.4	26.3

2.4. Solid-state NMR measurements

Solid-state ^{13}C NMR spectra were recorded at 100.613 MHz on a Bruker 400 MHz spectrometer at an ambient temperature of 298 K. Samples were packed into 4-mm zirconium oxide (ZrO) rotors. Cross-polarization and high-power decoupling were employed. A pulse delay of 7.0 s and a contact time of 5.0 ms were used in the CPMAS experiments. The magic angle spinning (MAS) rates were maintained at 4 kHz. Carbon chemical shifts were referenced to tetramethylsilane (TMS) by setting the high-frequency isotropic peak of solid adamantane to 38.56 ppm. The solid-state NMR data are given in Table 4.

2.5. IR and far-IR spectroscopy

A Perkin Elmer FTIR 180 spectrophotometer was used to collect the IR spectra for the ligands and the synthesized gold(III) complexes within the range 4000–400 cm^{-1}. Far-infrared spectra were recorded for the synthesized complexes **1** and **2** at room temperature with a 4 cm^{-1} resolution using polyethylene disks with a far-IR beam splitter.

2.6. UV–Vis spectroscopy

An aqueous solution of 0.5 mM $[(DACH)AuCl_2]Cl$ was prepared in phosphate buffer, pH 7.3, then its electronic spectrum was recorded using a Carry 100 UV–Vis Agilent spectrophotometer. An absorption band at 300 nm was observed for the prepared solution with an extinction coefficient 2180 L mol^{-1} cm^{-1} and this absorption could not be assigned to a d → d transition due to the high extinction coefficient; in comparison with Auric acid, this is a gold(III) to chlorido ligand charge transfer (MLCT). After 72 h the electronic spectrum for the same solution was collected and similar electronic behavior was observed, reflecting the stability of the prepared complexes under the prescribed conditions, as shown in Fig. S1.

2.7. X-ray crystallography

Suitable crystals of complexes **1** and **2** were obtained as pale yellow blocks and colorless rods from absolute ethanol, respectively. The intensity data were collected at 173 K (−100 °C) on a Stoe Mark II-Image Plate Diffraction System [34] equipped with a two-circle goniometer and using Mo Kα graphite monochromated radiation (λ = 0.71073 Å). The structures

Table 5
Crystal data and structure refinement details for complexes **1** and **2**.

Complex	**1**	**2**
CCDC deposit No.	1055595	1055495
Chemical formula	$2[C_6H_{14}N_2AuCl_2]^+\cdot 2(Cl)^-\cdot(H_2O)$	$[(C_6H_{14}N_2)_2Au]^{3+}\cdot 3(Cl)^-\cdot 4(H_2O)$
Molecular weight	853.03	603.76
Crystal system	monoclinic	monoclinic
Space group	$P2_1$	$P2_1$
T (K)	173	173
a (Å)	9.5692(5)	7.4766(3)
b (Å)	8.5645(5)	27.3859(10)
c (Å)	14.3950(8)	10.7744(5)
β (°)	95.369(4)	90.913(4)
V (Å^3)	1174.57(11)	2205.81(16)
Z	2	4
Radiation type	Mo Kα	Mo Kα
μ (mm^{-1})	13.17	7.06
Crystal size (mm)	0.40 × 0.38 × 0.35	0.45 × 0.35 × 0.30
Diffractometer	STOE *IPDS* 2 diffractometer	STOE *IPDS* 2 diffractometer
Absorption correction	Multi-scan (MULscanABS in PLATON; Spek, 2009)	Multi-scan (MULscanABS in PLATON; Spek, 2009)
$T_{minimum}$, $T_{maximum}$	0.251, 1.000	0.448, 1.000
No. of measured, independent and observed [$I > 2\sigma(I)$] reflections	16303, 4442, 4214	30420, 8309, 7854
R_{int}	0.142	0.079
$(\sin\theta/\lambda)_{max}$ (Å^{-1})	0.609	0.609
$R[F^2 > 2\sigma(F^2)]$	0.045	0.021
$wR(F^2)$	0.117	0.043
S	1.01	0.94
No. of reflections	4442	8309
No. of parameters	179	470
No. of restraints	1	21
Largest differences in peak and hole (e Å^{-3}) $\Delta\rho_{max}$, $\Delta\rho_{min}$ (e Å^{-3})	1.65, −2.38	1.08, −1.27
Absolute structural parameter	1.08, −1.27	−0.018(4)

were solved by direct methods with SHELXS-2014 [35]. The refinement and all further calculations were carried out with SHELXL-2014 [35]. The water H atoms were located from difference Fourier maps and refined using the distance restraint of O–H = 0.84(2) Å and with $U_{iso}(H) = 1.5U_{eq}(O)$. It was not possible to locate both H atoms on water molecules O7W and O8W for complex **2**.

The N- and C-bound H-atoms were included in calculated positions and treated as riding atoms: N–H = 0.91 Å and C–H = 0.99–1.00 Å with $U_{iso}(H) = 1.2U_{eq}(N,C)$. The non-H atoms were refined anisotropically using weighted full-matrix least-squares on F^2. A semi-empirical absorption correction was applied using the MULscanABS routine in PLATON [36]. Figs. 3–7, showing the crystal structures and crystal packing, were drawn using MERCURY software [37]. A summary of the crystallographic data of complexes **1** and **2** is given in Table 5.

2.8. In vitro cytotoxic assay for the synthesized gold(III) complexes

Complexes **1** and **2** were dissolved (10 mM) in DMSO and stored at −80 °C in volumes of 500 μL, or aliquots with volumes of 10 μL were taken and stored at −20 °C (then used once without refreezing). KR compounds were diluted in RPMI medium immediately before use. Cisplatin was purchased from Mayne Pharma. Culture medium with the same amount of drug-free DMSO was used as a negative control.

2.8.1. Cell lines and culture conditions

The classical Hodgkin lymphoma L-540 cell line was obtained from the German Collection of Microorganisms and Cell Cultures (Braunschweig, Germany). Human ovarian epithelial carcinoma-derived cancer cells A2780 and its cisplatin-resistant clone A2780cis were from Sigma, Inc. (St. Louis, MO, USA). The parent cisplatin-resistant subclone A2780cis was maintained by weekly treatment with 1 μM cisplatin [38]. Cells were cultured at 37 °C in 5% CO_2 in RPMI medium supplemented with 10% heat-inactivated FBS, 0.1% (w/v) L-glutamine and antibiotics (0.2 mg/ml penicillin and streptomycin).

2.8.2. Cell proliferation assay

For the assay, 4.0×10^3 A2780 and A2780cis cells were seeded in 96-well flat-bottomed microplates in RPMI medium (100 μL) and incubated at 37 °C in a 5% CO_2 atmosphere for 24 h (to allow cell adhesion) before drug testing. The medium was then removed and replaced with fresh medium containing the compounds to be tested at increasing concentrations (from 1 to 100 μM) at 37 °C for 72 h. Each treatment was performed in triplicate. Cell proliferation was assayed using the MTT assay. L-540 cells (2.0×10^5/ml) were seeded in 48-well plates and treated with increasing concentrations of the compounds. After 72 h, the number of viable cells was evaluated by a trypan blue dye exclusion assay. The IC_{50} values (i.e., the half maximal inhibitory concentration, representing the concentration of a substance required for 50% inhibition *in vitro*) were calculated using CALCUSYN software (Biosoft, Ferguson, MO, USA) [39]. Cell viability was imaged under an inverted microscope (Eclipse TS/100, Nikon) with a photomicrographic system (DS Camera Control Unit DS-L2).

2.8.3. Statistical analysis

Statistical analysis was performed using GRAPHPAD software. The significance of the differences was determined by Student's *t*-test for comparison between two groups. $P < 0.05$ was considered statistically significant, $^*P < 0.05$.

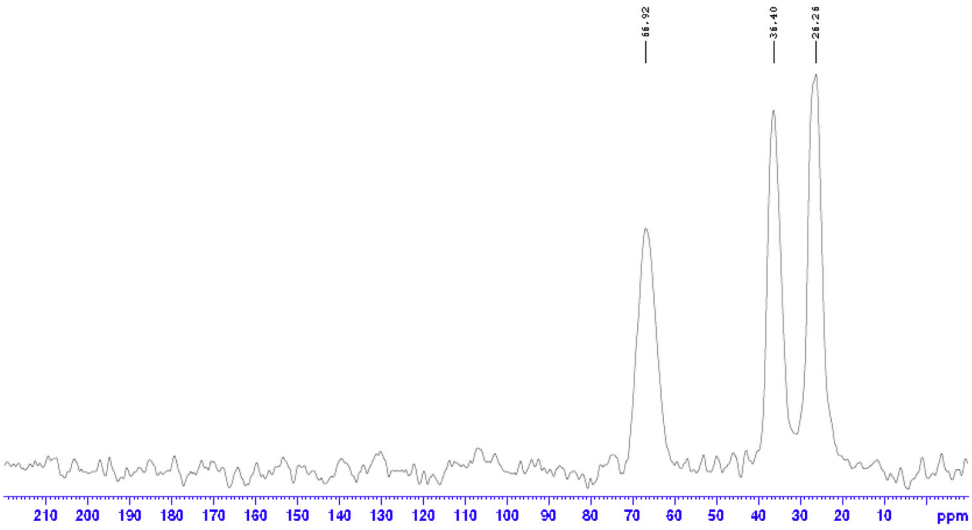

Fig. 1. Solid-state ^{13}C spectrum for complex 2 at a spinning rate of 4 kHz.

3. Results and discussion

3.1. Solution NMR

For both complexes **1** and **2**, Tables 2 and 3 clearly show that the observed number of ^{1}H and ^{13}C resonances is half of the expected number, which might indicate the presence of a C_2 centre of symmetry. All the cyclohexane protons showed downfield shifts relative to the free diaminocyclohexane ligand. At room temperature, the cyclohexane ring behaves as a rigid conformer upon complexation, which allows the axial and equatorial protons of the cyclohexane rings in **1** and **2** to be distinguished, as compared with the free diaminocyclohexane. These observed shifts can be explained by the donation of nitrogen lone pairs to the d orbitals of the gold(III) centre; this donation causes the nitrogen atoms to be more electron-deficient and makes the protons of the cyclohexane ring in **1** and **2** more deshielded, which shifts their resonances downfield, indicating that coordination takes place through the nitrogen atoms. The protons of the other rings are shifted downfield for the same reason. The observed resonances for complexes **1** and **2** are different. This variation is due to their different geometries.

Similar downfield shifts were observed for the ^{13}C resonances of the C1 and C2 atoms, adjacent to the amino groups. These two carbons become deshielded due to coordination through the nitrogen atoms, while the other carbons are shifted upfield.

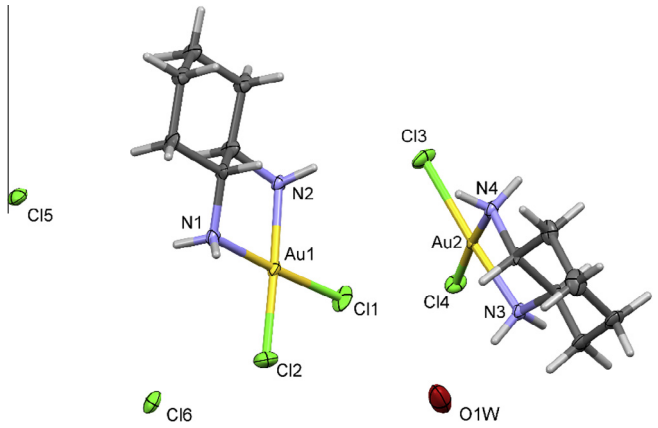

Fig. 2. A view of the molecular structure of complex **1**, with the atom labeling. The displacement ellipsoids are drawn at the 50% probability level.

Table 6
Selected bond lengths (Å) and bond angles (°) for complexes **1** and **2**.

Bond Lengths (Å)		Bond Angles (°)	
*Complex **1***			
Molecule 1			
Au1–Cl1	2.269(6)	Cl1–Au1–Cl2	91.4(2)
Au1–Cl2	2.261(5)	Cl1–Au1–N1	176.4(5)
Au1–N1	2.020(15)	Cl1–Au1–N2	92.8(5)
Au1–N2	2.059(16)	Cl2–Au1–N1	92.2(5)
		Cl2–Au1–N2	175.6(5)
		N1–Au1–N2	83.7(6)
Molecule 2			
Au2–Cl3	2.281(5)	Cl3–Au2–Cl4	93.71(17)
Au2–Cl4	2.275(5)	Cl3–Au2–N3	173.6(5)
Au2–N3	2.041(16)	Cl3–Au2–N4	92.6(5)
Au2–N4	2.028(15)	Cl4–Au2–N3	90.5(5)
		Cl4–Au2–N4	175.8(4)
		N3–Au2–N4	83.2(6)
*Complex **2***			
Molecule 1			
Au1–N1	2.039(6)	N1–Au1–N2	83.1(2)
Au1–N2	2.044(6)	N1–Au1–N3	179.2(2)
Au1–N3	2.041(6)	N1–Au1–N4	95.6(2)
Au1–N4	2.044(6)	N2–Au1–N3	97.7(2)
		N2–Au1–N4	178.2(3)
		N3–Au1–N4	83.6(2)
Molecule 2			
Au2–N7	2.048(6)	N7–Au2–N8	83.2(2)
Au2–N8	2.037(6)	N5–Au2–N8	177.4(3)
Au2–N5	2.021(8)	N5–Au2–N6	82.8(2)
Au2–N6	2.046(6)	N5–Au2–N7	97.6(2)
		N6–Au2–N7	178.0(3)
		N6–Au2–N8	96.5(2)

3.2. Solid-state NMR

In the solid-state ^{13}C NMR spectra, significant deshielding was observed (as shown in Fig. 1) for complex **2**, with similar trends in the chemical shifts for complex **1**, as given in Table 4. This similarity reflects the stability of the structures in solution as well as in the solid state.

3.3. FT-IR and far-IR spectroscopy

Both complexes **1** and **2** showed significant N-H stretching vibrations, with an observed blue-shift relative to the free ligand, within the range 3200–3500 cm^{-1}. This is due to coordination through an N atom and the formation of a five-membered ring with gold(III), which reduces the H bonding compared with the free amino groups in free DACH. The far-IR spectrum of complex **1** shows a clear vibration band at 367 cm^{-1}, which is assigned to Au–Cl stretching vibrations, with another band at 393 cm^{-1} for the Au–N bond [40]. Moreover, complex **2** lacks symmetric Cl–Au–Cl stretching vibrations at 352 and 367 cm^{-1}.

3.4. X-ray crystal structure

The crystal structure of complex **1** shown in Fig. 2. The compound crystallizes with two $[(C_6H_{14}N_2)AuCl_2]^+$ cations and two Cl^- anions in the asymmetric unit, together with a water molecule, for which it was not possible to locate the H atoms. The gold(III) ion is bonded to the two nitrogen atoms of the (1*R*,2*R*)-(+)-1,2-diaminocyclohexane ligand and two chloride ions in a distorted square planar geometry (Table 5). The Au–N bond distances in molecule 1 and molecule 2 are in the range 2.020(15)–2.059

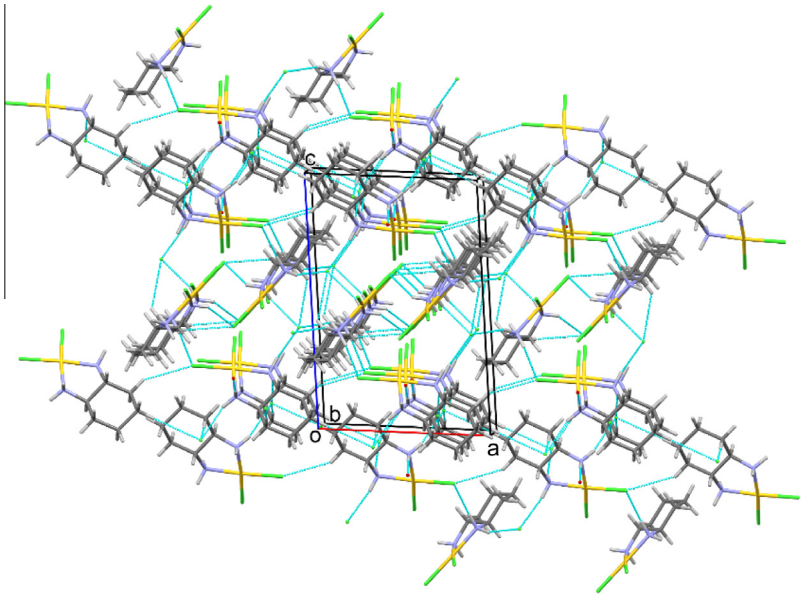

Fig. 3. Crystal packing of complex **1**, viewed along the *a*-axis.

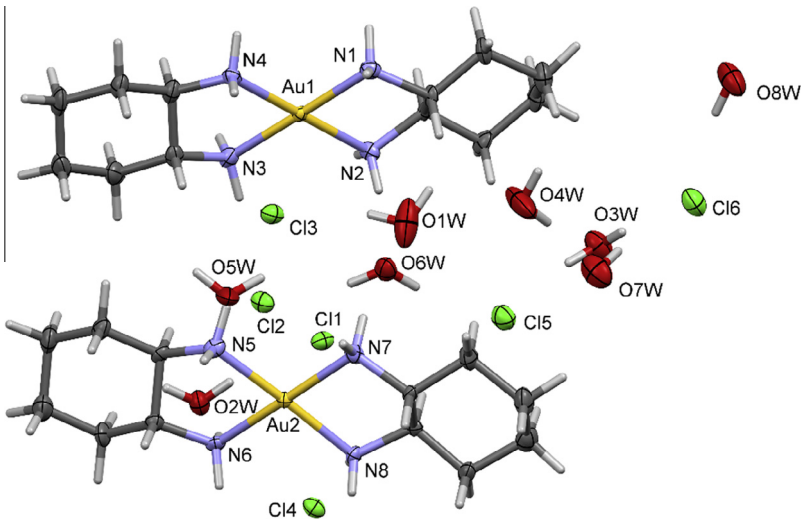

Fig. 4. A view of the molecular structure of complex **2** with the atom labeling. The displacement ellipsoids are drawn at the 50% probability level.

(16) Å, while the Au–Cl bond distances are in the range 2.261(5)–2.281(5) Å, as shown in Table 6. The Cl–Au–Cl and N–Au–N bond angles are 91.4(2)–93.71(17) and 83.2(6)–83.7(6)° for molecules 1 and 2, respectively. The Au–N bond distances in molecule 1 are significantly different from each other, whereas the Au–N bond distances in molecule 2 are very close to each other, but different from those of molecule 1. The N–Au–N bond angle values reflect the chelation strain of the diamine ligand. These values are similar to those found in other gold(III) complexes [41] and dichloro-(trans-(±)-1,2-diaminocyclohexane)-gold(III) chloride hydrates [40]. The cyclohexyl ring adopts a chair conformation. There is a square planar geometry around the Au(III) ion, resulting in five-membered ring formation. All the amine groups are engaged in hydrogen bonding with water molecules and the Cl^- counter ions. A water molecule is present in the crystal lattice. The metal complex molecules pack head to head, generating molecular chains along the *c*-axis, which in turn pack into layers parallel to the *ac*-plane (Fig. 3).

The X-ray structure of complex **2** is shown in Fig. 4. The compound crystallizes with two $[(C_6H_{14}N_2)_2Au]^{3+}$ cations, six Cl^-

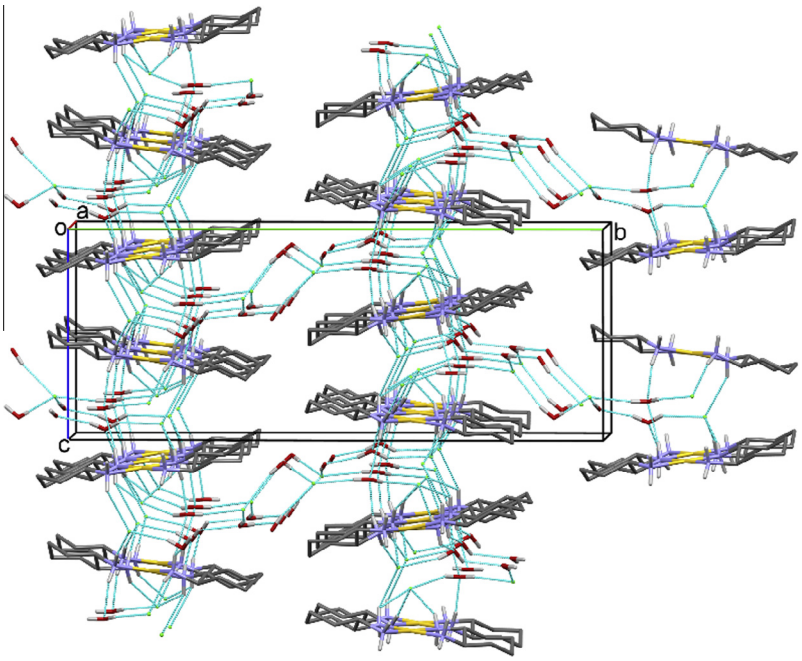

Fig. 5. Crystal packing of complex **2** viewed along the *a*-axis. Hydrogen bonds are shown as dashed lines (C-bound H atoms have been omitted for clarity).

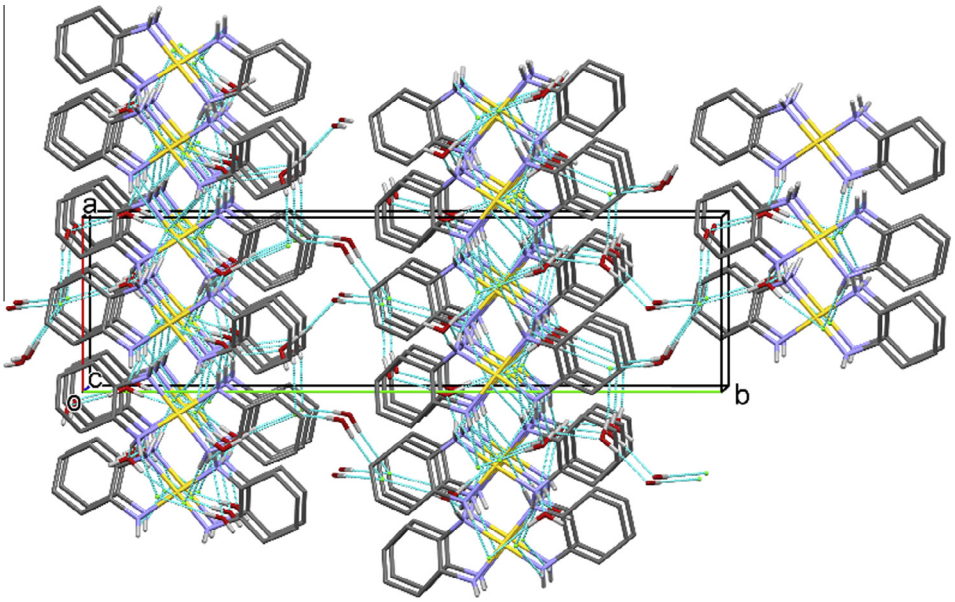

Fig. 6. Crystal packing of complex **2** viewed along the *c*-axis. Hydrogen bonds are shown as dashed lines (C-bound H atoms have been omitted for clarity).

anions and eight water molecules in an asymmetric unit. It was not possible to locate both H atoms on water molecules O7W and O8W. In both molecules, the metal ion is bonded to the four nitrogen atoms of two (1*R*,2*R*)-(+)-1,2-diaminocyclohexane ligands in a distorted square planar geometry. The Au–N bond distances are in the range 2.021(8)–2.048(6) Å, and the N–Au–N chelate bond angles are in the range 83.1(2)–83.6(2)° for molecules 1 and 2, as given in Table 6. These values are similar to those reported for [Au{trans-(±)-(1,2-DACH)}$_2$]Cl$_3$ [41] and bis (ethylene-1,2-diamine)-gold(III) tris(perrhenate) [42]. The cyclohexyl rings adopt a chair conformation. The square planar geometry and the five-membered ring strain impose torsion angles of 54.0(8)° for N1–C1–C2–N2 and of 58.3(8)° for N3–C7–C8–N4 in molecule 1, and of 52.4(8)° for N5–C13–C14–N6 and of 50.6 (8)° for N7–C19–C20–N8 in molecule 2. The amine group hydrogen atoms are involved in hydrogen bonding interactions with Cl^- counter ions and water molecules, generating a three-dimensional hydrogen bonding network, as shown in Figs. 5 and 6.

3.5. In vitro cytotoxic assay for the synthesized complexes

We evaluated the *in vitro* antiproliferative activity of complexes **1** and **2** in the classical Hodgkin lymphoma-derived cell line L-540 (Fig. 7). Exposure of L-540 cells to increasing concentrations of both gold complexes resulted in a dose-dependent cytotoxic activity, as shown in representative microphotographs (Fig. 7A). Complex **2** exhibited a more potent inhibition of cell growth compared to complex **1** (Fig. 7A and B), as evaluated by the trypan blue assay. Complex **2** was 7-fold more active than compound **1**, with IC_{50} values of 9.8 and 70.4 μM, respectively (Fig. 7B).

The cytotoxic activities of the gold complexes **1** and **2** were also evaluated in the ovarian carcinoma-derived cell line A2780 and in its cisplatin-resistant clone (A2780cis) using an MTT assay. For comparison purposes, the cisplatin activity was evaluated under the same experimental conditions. Both compounds inhibited proliferation in a dose-dependent manner (Fig. 8A and B). Again, complex **2** exhibited a more potent inhibition of cell growth as compared to complex **1** in both A2780 (Fig. 8C) and A2780cis cells (Fig. 8D). The IC_{50} values of complex **1** were 61.3 μM for A2780cis and 15.7 μM for A2780 cells, and for complex **2**, the IC_{50} values were 31.1 μM for A2780cis and 6.98 μM for A2780 (Table 7). The IC_{50} values for cisplatin in A2780cis and A2780 were 17.6 and 1.8 μM, respectively, showing a 9.7-increase in resistance (fold resistance) to cisplatin in A2780cis compared with A2780 (Table 7). Although the IC_{50} values for both gold complexes were higher than those for cisplatin in A2780 and A2780cis cells, the fold-resistances of both complexes were approximately twofold lower than that of cisplatin (Table 7).

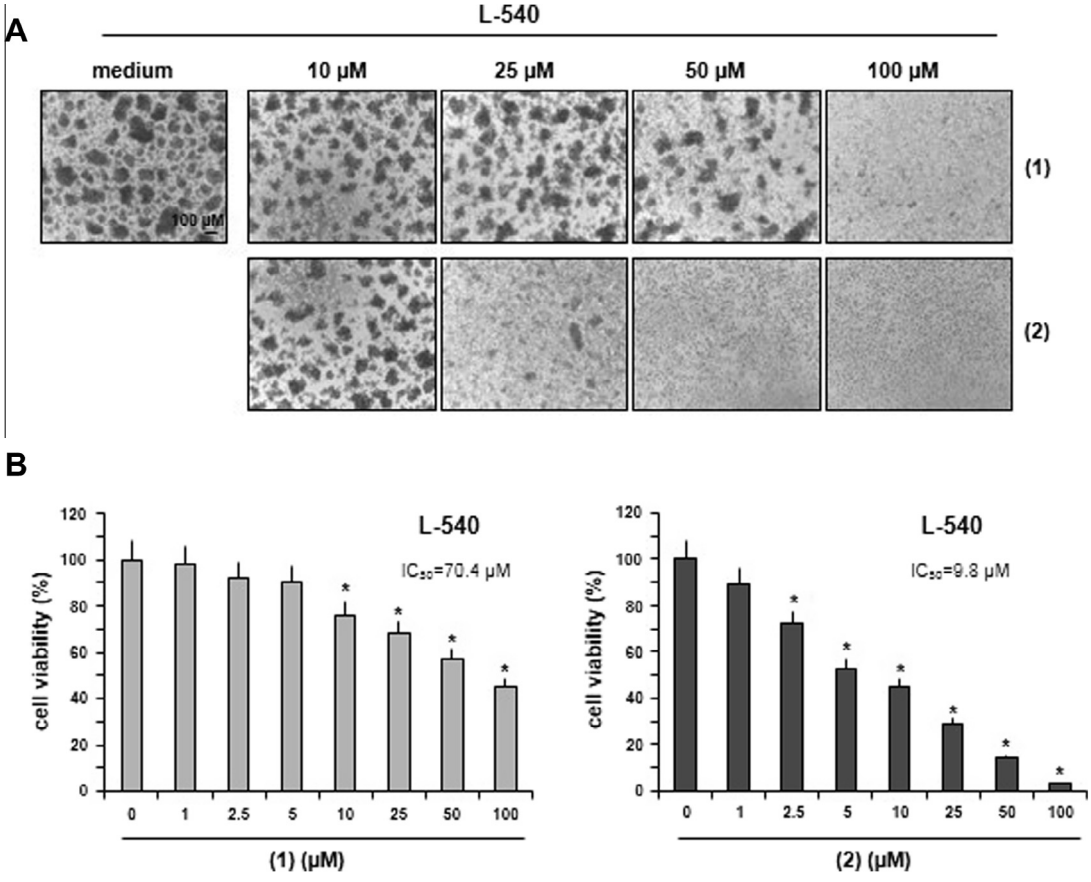

Fig. 7. Antiproliferative activity of gold complexes **1** and **2** in classical Hodgkin lymphoma L-540 cells. Cells were cultured (2.0×10^5/ml) in the presence of increasing drug concentrations (1–100 μM). After 72 h (A), representative microphotographs were captured using an inverted microscope (phase contrast microphotographs; original magnification 4×). (B) Histograms showing the percentage of living cells, evaluated by trypan blue dye exclusion assay. IC_{50} values, calculated using the CALCUSYN software, are reported in the graphs. Data are expressed as the mean ± SEM of three independent experiments. $^*P < 0.05$ gold complex vs. control medium.

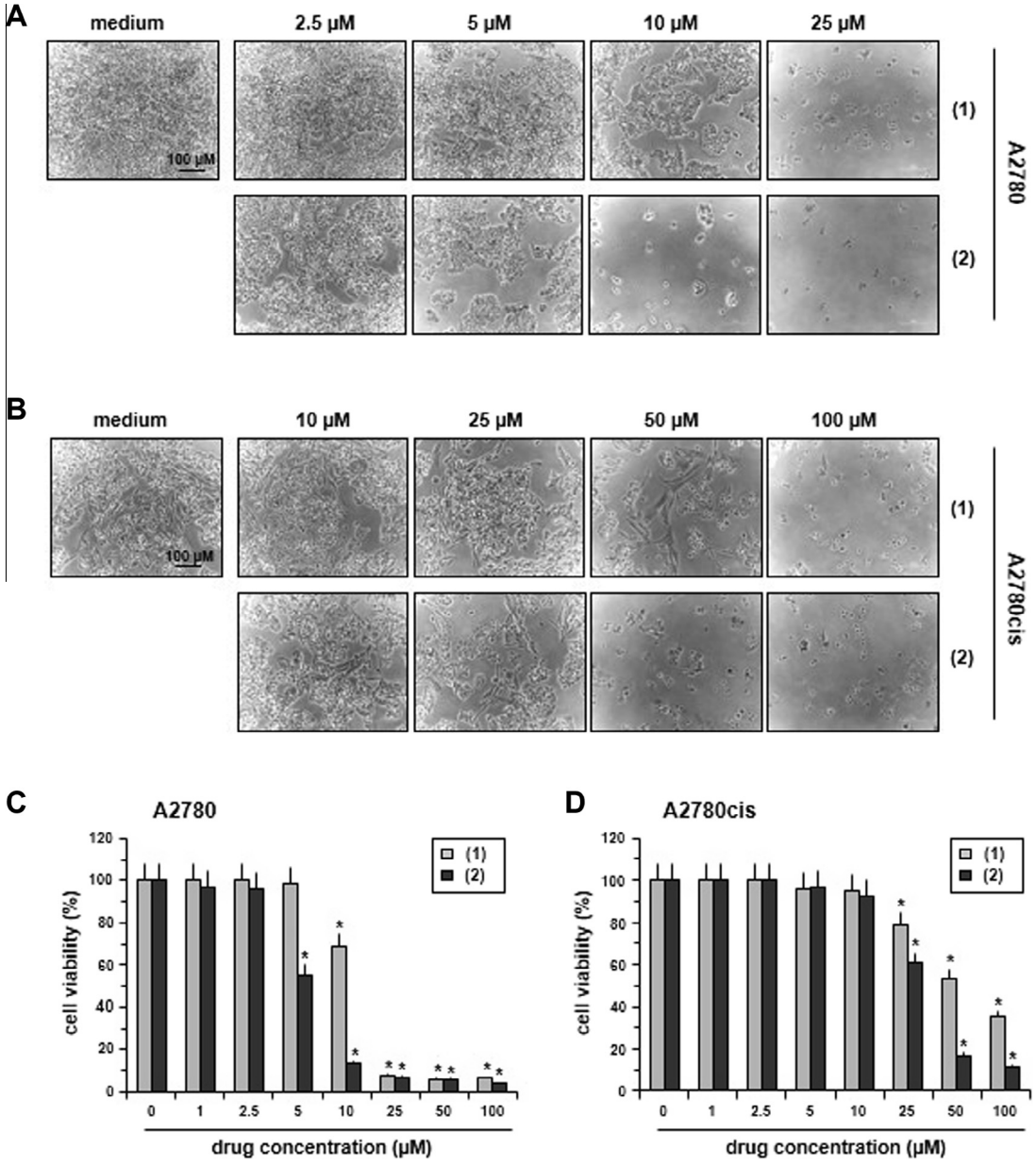

Fig. 8. Antiproliferative activity of gold complexes **1** and **2** in ovarian carcinoma-derived cell lines. A2780 and its cisplatin-resistant clone A2780cis were cultured (4.0×10^3) in the presence of increasing concentrations of drug (1–100 μM). After 72 h of treatment (A and B), representative images were captured using an inverted microscope (phase contrast microphotographs; original magnification 10×). (C and D) Histograms showing the percentage of living cells evaluated by MTT assay. Data are expressed as the mean ± SEM of three independent experiments. $^*P < 0.05$ gold complex vs. control medium.

Table 7
Growth inhibition by complexes **1** and **2** in A2780, A2780cis and L-540 cancer cells.

Complex	L-540	IC_{50} (μM)		Fold resistance A2780cis/A2780ratio
		A2780	A2780cis	
Cisplatin	2.5 ± 0.1	1.8 ± 0.1	17.6 ± 1.5	9.77
1	70.4 ± 4.5	15.7 ± 1.4	61.3 ± 5.5	3.90
2	9.8 ± 0.8	6.9 ± 0.6	31.1 ± 2.8	4.45

Cell lines were exposed to increasing concentrations of complex **1**, complex **2** and cisplatin. After 72 h of exposure, viable cells were evaluated by MTT assay. The results represent the mean ± SEM of three replicate wells from three independent experiments. IC_{50} values were calculated using CALCUSYN software and compared with the reference drug cisplatin.

Altogether these results point out the higher cytotoxic potential of compound (**2**) respect to compound (**1**) and the lower fold-resistance of both compounds respect to cisplatin.

4. Conclusions

Here, we report the synthesis, characterization, X-ray structures and *in vitro* cytotoxic activity of two gold(III) complexes that contain the 1(*R*),2(*R*)-diaminocyclohexane ligand against the ovarian carcinoma-derived cell line A2780 and its cisplatin-resistant clone (A2780cis) using an MTT assay; both complexes showed high cytotoxic potentials. Although the IC_{50} values of the gold(III) complexes (**1** and **2**) were higher than cisplatin in A2780 and A2780cis cells, they showed excellent cytotoxic activity against with the ovarian cancer cell line and its cisplatin-resistant clone. The *in vitro* cytotoxic activity of gold(III) complexes (**1** and **2**) against the cisplatin-resistant A2780cis cells makes them potential anticancer agents for further investigation.

Acknowledgement

This project was funded by the National Plan for Science and Innovation (MARIFAH)–King Abdulaziz City for Science and Technology (KACST) through the Science and Technology Unit at King Fahd University of Petroleum and Minerals (KFUPM) of Saudi Arabia, award No. 14-MED64-04.

Appendix A. Supplementary data

CCDC 1055595 and 1055495 contains the supplementary crystallographic data for compounds **1** and **2**, respectively. These data can be obtained free of charge via http://www.ccdc.cam.ac.uk/conts/retrieving.html, or from the Cambridge Crystallographic Data Centre, 12 Union Road, Cambridge CB2 1EZ, UK; fax: (+44) 1223-336-033; or e-mail: deposit@ccdc.cam.ac.uk.

Supplementary data associated with this article can be found, in the online version, at http://dx.doi.org/10.1016/j.poly.2015.10.029.

References

[1] S. Medici, M. Peana, V.M. Nurchi, J.I. Lachowicz, G. Crisponi, M.A. Zoroddu, Coord. Chem. Rev. 284 (2015) 329.
[2] A. Casini, G. Kelter, C. Gabbiani, M.A. Cinellu, G. Minghetti, D. Fregona, H.-H. Fiebig, L. Messori, J. Bio Inorg. Chem. 14 (2009) 1139.
[3] S.H. van Rijt, P.J. Sadler, Drug Discov. Today 14 (2009) 1089.
[4] X. Wang, Z. Guo, Dalton Trans. (2008) 1521.
[5] L. Galluzzi, L. Senovilla, I. Vitale, J. Michels, I. Martins, O. Kepp, M. Castedo, G. Kroemer, Oncogene 31 (2012) 1869.
[6] S. Nobili, E. Mini, I. Landini, C. Gabbiani, A. Casini, L. Messori, Med. Res. Rev. 30 (2009) 550.
[7] E.M. Nagy, L. Ronconi, C. Nardon, D. Fregona, Mini Rev. Med. Chem. 12 (2012) 1216–1229.
[8] I. Ott, Coord. Chem. Rev. 253 (2009) 1670.
[9] C.P. Tan, Y.Yi. Lu, L.N. Ji, Z.-W. Mao, Metallomics 6 (2014) 978.
[10] M.A. Cinellu, L. Maiore, M. Manassero, A. Casini, M. Arca, H.-H. Fiebig, G. Kelter, E. Michelucci, G. Pieraccini, C. Gabbiani, L. Messori, A.C.S. Med, Chem. Lett. 1 (2010) 336.
[11] A. Bindoli, M.P. Rigobello, G. Scutari, C. Gabbiani, A. Casini, L. Messori, Coord. Chem. Rev. 253 (2009) 1692.
[12] A. Casini, C. Hartinger, C. Gabbiani, E. Mini, P.J. Dyson, B.K. Keppler, L. Messori, J. Inorg. Biochem. 102 (2008) 564.
[13] V. Milacic, D. Fregona, Q.P. Dou, Histol. Histopathol. 23 (2008) 101.
[14] M.W. Whitehouse, Inflammopharmacology 16 (2008) 107.
[15] G.G. Graham, M.W. Whitehouse, G.R. Bushell, Inflammopharmacology 16 (2008) 126.
[16] M. Altaf, A.A. Isab, J. Vančo, Z. Dvořák, Z. Trávníček, H. Stoeckli-Evans, RSC Adv. 5 (2015) 81599.
[17] M. Celegato, C. Borghese, N. Casagrande, M. Mongiat, X.U. Kahle, A. Paulitti, M. Spina, A. Colombatti, D. Aldinucci, Blood 126 (2015) 1394.
[18] L. Giovagnini, L. Ronconi, D. Aldinucci, D. Lorenzon, S. Sitran, D. Fregona, J. Med. Chem. 48 (2005) 1588.
[19] S.S. Al-Jaroudi, M. Altaf, A.A. Al-Saadi, A.-N. Kawde, S. Altuwaijri, S. Ahmad, A.A. Isab, Biometals 28 (2015) 827.
[20] S.S. Al-Jaroudi, M. Monim-ul-Mehboob, M. Altaf, A.A. Al-Saadi, M.I.M. Wazeer, A.A. Isab, Biometals 27 (2014) 1115–1136.
[21] D. Saggioro, M.P. Rigobello, L. Paloschi, A. Folda, S.A. Moggach, S. Parsons, L. Ronconi, D. Fregona, A. Bindoli, Chem. Biol. 14 (2007) 1128.
[22] G. Sava, A. Bergamo, P.J. Dyson, Dalton Trans. 40 (2011) 9069.
[23] L. Kelland, Nat. Rev. Cancer 7 (2007) 573.
[24] A.V. Vujačić, J.Z. Savić, S.P. Sovilj, K. Mészáros Szécsényi, N. Todorović, M.Ž. Petković, V.M. Vasić, Polyhedron 28 (2009) 593.
[25] T. Kolev, B.B. Koleva, S.Y. Zareva, M. Spiteller, Inorg. Chim. Acta 359 (2006) 4367.
[26] J. Zou, Z. Guo, J.A. Parkinson, Y. Chen, P.J. Sadler, Chem. Commun. 8 (1999) 1359.
[27] J.A. Cuadrado, W. Zhang, W. Hang, V. Majidi, J. Environ. Monit. 2 (2000) 355.
[28] P.L. Witkiewicz, C.F. Shaw, III, J. Chem. Soc., Chem. Commun. (1981) 1111.
[29] S. Zhu, W. Gorski, D.R. Powell, J.A. Walmsley, Inorg. Chem. 45 (1981) 2688.
[30] B.Đ. Glišić, M.I. Djuran, Z.D. Stanić, S. Rajković, Gold Bull. 47 (2014) 33.
[31] M.D. Durović, Z.D. Bugarčić, F.W. Heinemann, R. van Eldik, Dalton Trans. 43 (2014) 3911.
[32] S.S. Al-Jaroudi, M. Fettouhi, M.I.M. Wazeer, A.A. Isab, S. Altuwaijri, Polyhedron 50 (2013) 434.
[33] S.S. Al-Jaroudi, M. Monim-ul-Mehboob, M. Altaf, M. Fettouhi, M.I.M. Wazeer, S. Altuwaijri, A.A. Isab, New J. Chem. 38 (2014) 3199.
[34] Stoe, Cie, X-AREA & X-RED32, Stoe & Cie GmbH, Darmstadt, Germany, 2009.
[35] G.M. Sheldrick, Acta Crystallogr. A64 (2008) 112.
[36] A.L. Spek, Acta Crystallogr. D65 (2009) 148.
[37] C.F. Macrae, I.J. Bruno, J.A. Chisholm, P.R. Edgington, P. McCabe, E. Pidcock, L. Rodriguez-Monge, R. Taylor, J. van de Streek, P.A. Wood, J. Appl. Crystallogr. 41 (2008) 466.
[38] N. Casagrande, M. Celegato, C. Borghese, M. Mongiat, A. Colombatti, D. Aldinucci, Clin. Cancer Res. 20 (2014) 5496.
[39] T.C. Chou, P. Talalay, Adv. Enzyme Regul. 22 (1984) 27.
[40] R. Parish, J.P. Wright, R.G. Pritchard, J. Organomet. Chem. 596 (2000) 165.
[41] M. Monim-ul-Mehboob, M. Altaf, M. Fettouhi, A.A. Isab, M.I.M. Wazeer, M.N. Shaikh, S. Altuwaijri, Polyhedron 61 (2013) 225.
[42] E.V. Makotchenko, I.A. Baidina, J. Struct. Chem. 52 (2011) 572.